Published in final edited form as:

Exp Brain Res. 2016 November ; 234(11): 3245–3257. doi:10.1007/s00221-016-4722-5.

Vestibular ablation and a semicircular canal prosthesis affect postural stability during head turns

Lara A. Thompson[3,4], **Csilla Haburcakova**[1,3], and **Richard F. Lewis**[1,2,3,4]

[1]Department of Otolaryngology, Harvard Medical School, Boston MA

[2]Department of Neurology, Harvard Medical School, Boston MA

[3]Jenks Vestibular Physiology Laboratory, Massachusetts Eye and Ear Infirmary, Boston MA

[4]Harvard University - Massachusetts Institute of Technology (MIT), Division of Health Sciences and Technology, Cambridge, MA

Abstract

In our study, we examined postural stability during head turns for two rhesus monkeys: one, single animal study contrasted normal and mild bilateral vestibular ablation and a second animal study contrasted severe bilateral vestibular ablation with and without prosthetic stimulation. The monkeys freely stood, unrestrained on a balance platform and made voluntary head turns between visual targets. To quantify each animals' posture, motions of the head and trunk, as well as torque about the body's center-of-mass, were measured. In the mildly ablated animal, we observed less foretrunk sway in comparison to the normal state. When the canal prosthesis provided electric stimulation to the severely ablated animal, it showed a decrease in trunk sway during head turns. Because the rhesus monkey with severe bilateral vestibular loss exhibited a decrease in trunk sway when receiving vestibular prosthetic stimulation, we propose that the prosthetic electrical stimulation partially restored head velocity information. Our results provide an indication that a semicircular canal prosthesis may be an effective way to improve postural stability in patients with severe peripheral vestibular dysfunction.

Keywords

vestibular; posture; balance; prosthesis; implant

Introduction

Approximately 8 million American adults have chronic balance impairments due to damage in the peripheral vestibular system (NIDCD 2008). When vestibulospinal inputs are

Corresponding author: Lara A. Thompson, University of the District of Columbia, 4200 Connecticut Avenue NW, 42-213F, Washington DC, 20008, Tel: 202 274 5046; Fax: 202 274 6232, lara.thompson@udc.edu.

Disclosures

None

All applicable international, national, and/or institutional guidelines for the care and use of animals were followed. All procedures performed in studies involving animals were in accordance with the ethical standards of the institution or practice at which the studies were conducted.

impaired or absent, patients suffer from imbalance and have an increased risk of falls. While the brain may partially compensate for a relatively mild loss of peripheral vestibular function, many patients with severely impaired vestibular function will remain permanently debilitated (i.e., suffer from oscillopsia (blurred vision), vertigo, and imbalance). Furthermore, the postural compensation for different levels of peripheral vestibular dysfunction for destabilizing events, such as heads turns, remains uncertain. Therefore, it is clear that there is a pressing need to better understand how various levels of peripheral vestibular dysfunction affect posture, as well as to develop new therapeutic approaches that will improve postural control in patients suffering from imbalance due to severe peripheral vestibular hypofunction.

Currently, there are two general therapeutic approaches: *non-invasive* "sensory substitution" devices and *invasive* semicircular canal "prostheses" that sense angular head motion in a manner that recapitulates the normal canals and supplies this information to the brain via electrical stimulation of the canal afferents. Examples of sensory substitution devices currently being studied are all based on sensing body tilt and providing feedback via a non-vestibular pathway, such as tactile stimulation applied to the torso (e.g., Peterka et al. 2006), audio biofeedback (e.g., Dozza et al. 2005) or electrical stimulation of the tongue (e.g., Bach-y-Rita and Kercel 2003; Tyler et al. 2003). While these approaches may augment posture reflexes, they cannot fully emulate vestibular function nor do they restore the visual reflexes linked to normal vestibular function (e.g., the vestibuloocular reflex (VOR)).

Invasive approaches ("vestibular prostheses" or "vestibular implants") electrically stimulate the primary vestibular canal afferents and are aimed at restoring vestibular function. The vestibular system responds to head movements that are both angular (via the semicircular canals) and linear (via the otolith organs). Although a prosthesis that restores full vestibular function to both the otoliths and the semicircular canals would be ideal, this technology is not yet feasible—More specifically, directing electrical stimulation to the otoliths is hindered by the complex orientation of their hair cells. Instead, past and current investigations have involved the use of prototype semicircular canal prostheses aimed at restoring head rotational cues. Among the first were Gong and Merfeld (2002) who created a one-dimensional prosthesis that restored the angular VOR in a guinea pig with a plugged semicircular canal. To explore the effects of the prosthesis on eye movements in non-human primates, squirrel monkeys with severe vestibular dysfunction have been also been used (e.g., Lewis et al. 2010; Merfeld et al. 2007). Furthermore, the development of a three-dimensional prosthesis used to restore rotational cues to three semicircular canals has been investigated in chinchillas (e.g., Della Santina et al. 2006; Fridman et al. 2010) and rhesus monkeys (e.g., Chiang et al. 2011). Nie et al. (2013) investigated the effects of vestibular prosthesis stimulation pulse trains that were unmodulated (constant current and rate), amplitude modulated (PAM), or rate modulated (PRM) on normal rhesus monkey eye movements. The prosthesis used was developed utilizing an existing platform for cochlear implants. Two monkeys that underwent similar implantation surgeries had eye movement responses that were induced by PAM versus PRM pulses. The direction of the eye movement was in agreement with the site stimulated in the vestibular labyrinth. Their eye movement results were encouraging and suggested that it is possible to use either PAM or PRM modulations to encode head movement signals in future vestibular implants. Mitchell

et al. (2013) explored the effects of a unilateral, 3D canal prosthesis on rhesus monkeys' head movements. Two animals were studied: One (normal) rhesus monkey was implanted with its canals intact; another animal that had received bilateral intratympanic gentamicin that yielded profoundly reduced VOR responses, consistent with severe vestibular damage. Animals were alert and seated in a primate chair while in complete darkness during experiments with their heads unrestrained. Mitchell et al. (2013) found that that head movement amplitudes and velocities increased with increasing (prosthesis) current amplitudes. This study demonstrated that a rhesus monkey with a normal vestibular system using a vestibular prosthesis had canal-specific, electrically evoked eye movements. However, further work is required to determine effects for natural activities such as gaze shifts, free-standing unseated balance, and locomotion.

Aside from the above animal studies, there were also a limited number of vestibular prosthesis eye movement investigations in humans. Wall et al. (2007) showed that electric stimulation to the human end organ or its vestibular nerve branches is capable of eliciting a nystagmic eye movement response. Three human subjects were provided electric stimulation of their posterior ampullary nerve, which was surgically exposed under local anesthesia. The stimulus was a multiphasic, charge-balanced train of electric pulses. In all subjects, a pulse repetition rate of 200 pulses per second produced a robust vertical nystagmus. This was an essential step in demonstrating the feasibility of a vestibular prosthesis that utilized electric stimulation in human test subjects. Guyot et al. (2011) investigated if a vestibular prosthesis (prototype derived from a custom-modified Med-E1 cochlear implant) could restore a baseline or "rest" activity in the vestibular pathways and then modulate it according to the direction and velocity of head movements. This study showed that a single, human subject that was bilaterally deaf with bilateral vestibular loss could adapt to continuous electrical stimulation of the vestibular system, and that it was possible to elicit artificial smooth oscillatory eye movements via modulation of the prosthesis' electric stimulation. Although this is a case study of one patient, the results suggest that humans can potentially adapt to electrical stimulation of the vestibular system with limited discomfort. Once the subject is in the adapted state, the electrical stimulation can be modulated to artificially elicit smooth eye movements. Gulob et al. (2014) investigated the effects of a vestibular prosthesis implanted in (one) human on canal-specific eye movements. This study showed that implantation of all canals is technically feasible. For the one subject (a 56 year old male suffering from Meniere's disease) used for this study, the prosthesis resulted in the subject having electrically evoked eye movements that were robust. For Meniere's patients considering destructive therapeutic procedures (e.g., intratympanic gentamicin, labyrinthectomy, and vestibular nerve section), a vestibular prosthesis could pose a favorable alternative.

While previous studies have investigated the effects of invasive semicircular canal prostheses *almost exclusively* on eye movements (referenced above) and the perception of earth-vertical (Lewis et al. 2013), their influences on posture have not been examined until recently. It has been shown that electrical stimulation of the peripheral vestibular system causes postural responses. Galvanic vestibular stimulation (GVS), a simple method that allows probing of posture effects to altered vestibular signals, has been studied in humans (e.g., Fitzpatrick and Day 2004). Fitzpatrick and Day (2004) showed that GVS stimulation affected human body sway magnitude and direction, with greater stimulation current yielding higher tilt

amplitudes. However, unlike natural stimuli, GVS has no directionality and the *entire population* of susceptible afferents are stimulated, regardless of the alignment of the hair cells they innervate. These limitations are overcome by direct stimulation of the ampullary nerve afferents with the canal prosthesis we have developed and studied here. Although the prosthesis only stimulates the canals, there is considerable evidence that the angular velocity information transduced by the canals is integrated by the brain to estimate head orientation relative to gravity (e.g. Lewis et al., 2013), which is almost certainly a critical element of the postural control system.

More recently, the acute effects of human postural responses to electrical stimulation of canal afferents were studied by Phillips and colleagues (Phillips et al. 2013), and they demonstrated that canal stimulation elicited postural responses with directional selectivity, with the sway magnitude modulating with the amplitude of the current. Interestingly, eye movements were not consistent with postural responses as the direction of the elicited eye movements changed as a function of stimulation current level, but the direction of the postural response did not change. However, this study serves as an initial step that demonstrates the potential feasibility of a canal prosthesis to modulate, not only eye movements, but postural stability in human subjects.

Although the effects of the vestibular prosthesis on eye movements have been rigorously studied, the effects of a vestibular prosthesis on posture and balance has been understudied and requires more investigation. In particular, the exploration of freely-standing balance for a head turn task for different levels of vestibular function, including the use of a prototype vestibular prosthesis, have been not studied in neither animals nor humans. This paper set out to contribute new knowledge, forming a baseline from which future human and animal research will be built upon.

In our study, we investigated our hypothesis that an animal with mild vestibular damage would be able to stabilize its posture during head turns. However, an animal with severe vestibular loss would require a therapeutic aid (a vestibular prosthesis) to stabilize its posture. We report the results from two animals as distinct studies: one single animal study contrasting normal and mild bilateral hypofunction (mBVH) and a second animal study contrasting severe bilateral hypofunction (sBVH) and sBVH with prosthetic stimulation (sBVH + STIM-ON).

The foretrunk sway of rhesus monkeys was examined while they stood in their normal, quadrupedal stance on a balance platform, and made voluntary head turns between visual targets. We used this approach because it is common knowledge that humans with severe bilateral vestibular dysfunction become unstable when the turn their heads rapidly, and because head turns generate instability in vestibulopathic (quadrupedal) cats (Stapley et al. 2006). During head turns, we examined how different degrees of peripheral vestibular damage affected postural sway and evaluated the potential utility of a one-dimensional canal prosthesis to stabilize posture. Since the quadrupedal animal had a more narrowed mediolateral foot spacing (related to roll movements) compared to anterior-posterior foot-spacing (related to pitch movements), and also due to the sway in the roll plane for humans

being correlated with fall risk (Rogers and Mille 2003), we focused specifically on foretrunk stability in roll (i.e., rotations of the horizontal trunk about an earth-horizontal axis).

We proposed the following hypotheses: a) mild bilateral vestibular ablation could adequately be compensated for (e.g., postural sway during head turns would be approximately normal); and b) the canal prosthesis stimulation could help stabilize postural sway in the severe vestibular ablated animal.

Methods

Experiments were approved by the Institutional Animal Care Committee and were in accordance with USDA guidelines. Two juvenile female rhesus monkeys were used in these experiments: monkey *M* (6.7 kg) and monkey *S* (7.9 kg). In both animals, vestibular ablation was induced by aminoglycoside administration. Monkey *M*'s posture was studied prior to vestibular ablation (we will call this state "normal"), but was also studied in a mildly ablated state (i.e., the mild bilateral vestibular hypofunction, or "mBVH", state). Monkey *S*'s posture was studied in the severely ablated state (i.e., the severe bilateral vestibular hypofunction, or "sBVH", state) and a severely ablated plus (vestibular) prosthetic-stimulated state (or "sBVH+ STIM"). Monkey *S* had a unilateral electrode implanted in the right posterior canal (the characteristics of the vestibular prosthesis are described briefly below).

Using standard methods (Judge et al. 1980), for each animal a frontal and torsional eye coil was implanted in one eye. The VOR was measured with a CNC search coil system. A head-bolt was implanted to immobilize the head during VOR testing and to hold the juice reward tube used while conducting the experiments.

Quantifying vestibular function

Vestibular ablation was induced with a combination of intratympanic (IT) gentamicin and systemic intramuscular (IM) streptomycin injections. Monkey *S* received three cycles of bilateral IT gentamicin using standard procedures (Minor 1999) followed by two cycles of IM streptomycin (350 mg/kg/day for 21 days); Monkey *M* received six cycles of IT gentamicin in both ears followed by 3 cycles of IM streptomycin using the same dosing schedule. The animal's VOR was characterized in the sBVH state after the dosing schedule was complete and after the prosthetic implantation had taken place.

Since the posture study focused on roll tilt of the foretrunk about an earth-horizontal axis and the monkey's head was approximately upright during postural testing (and therefore rotated about the same roll axis as the body), we quantified the extent of peripheral vestibular damage by measuring the VOR response during en-bloc head and body roll rotation about an earth-horizontal axis while the head was fixed. This motion paradigm modulates both canal and otolith activity concurrently, thereby providing an estimate of damage in both types of vestibular end-organs. We measured the VOR using sinusoidal roll rotation at 0.5 Hz, with a peak velocity of 20 deg/s.

Vestibular prosthesis

The details of the prosthesis surgery, design and implementation have been previously published (Gong and Merfeld 2002; Lewis et al. 2010; Lewis et al. 2013; Merfeld et al. 2007) and will only be described briefly here. Our study utilized a unilateral, one-dimensional, semicircular canal prosthesis in which the electrode was placed in the ampulla of the right posterior canal of monkey *S*. The orientation of the prosthesis sensor was in the plane of the implanted, right posterior canal. The electrode wire was routed to an electronics housing (head cap) located near the animal's head bolt. The surgery for placing the unilateral vestibular prosthesis may have caused additional vestibular damage. However, monkey *S*' posture was studied only after both the ablation via aminogylcocides and the prosthesis surgery had taken place.

The one-dimensional prosthesis sensed high-pass filtered head velocity (~0.03 Hz cutoff frequency, time constant of 5 s), to mirror the system dynamics of the mechanisms associated with a normal rhesus monkey semicircular canal. The filtered head velocity was used to modulate the current pulse rate of the electric stimulus so that increased (or decreased) head velocity resulted in increased (or decreased) spike rate, similar to the normal physiology of the canal and ampullary nerve. The tonic, baseline pulse rate was 250 Hz with pulse amplitude in the range of 90 μA, with 200 μs pulse duration. The rate was modulated to provide a bidirectional cue (i.e., head turns that were ipsilateral to the stimulating electrode increased the rate of stimulation while head turns that were contralateral to the stimulating electrode decreased rate of stimulation). The modulation itself was based on a hyperbolic tangent function that saturated at higher angular velocities (past +/− 300 deg/s), but was approximately linear for mid-range velocities.

Balance platform

Rhesus monkeys are habitual quadrupeds and were examined in their natural, quadrupedal stance. Fig. 1 shows a schematic drawing of the rear view (a & b) and top view (c) of the balance platform which consisted of four footplates (6 in × 2 in × 2.5 in/footplate) each covered with a thin, hard rubber. Based on the two monkeys' foretrunk lengths, the anterior-posterior set of footplates were positioned to L = 29 cm apart. The stance width (medial-lateral distance) was set at w = 9 cm, which was narrower than the animal's natural stance width and the narrowest possible setting for the balance platform. The purpose of the narrowed stance width was to decrease the animal's base-of-support and therefore increase the animal's difficulty-level for balancing on the platform.

During the experiments, visual orientation cues were limited by black draping of the surrounding visual field and dim lighting. Specifically, the visual environment consisted of black draping on the wall in front of and to the sides of the balance platform. Black draping surrounded the footplates of the platform and black flooring was at the base of the platform itself. Furthermore, experiments were all conducted in dim ambient lighting. A fan was turned on high to provide ambient noise, masking any sounds that may have otherwise startled the animal.

Because the quadrupedal monkey had a more narrowed stance in the mediolateral (side-to-side) direction than in the anterior-posterior (front-to-back) direction, the animal showed greater instability in the mediolateral direction. Furthermore, we were most interested in the animal's foretrunk sway in the roll plane (i.e., rotations of the foretrunk about an earth-horizontal axis).

The animal was trained to stand free of human or mechanical restraint on the balance platform in order to receive a juice reward. The juice reward system was connected to the animal's headcap, and the reward tubing was routed to the animal's mouth by a non-rigid tube. This configuration was used so that the animal could freely rotate its head towards the illuminated target.

Head Turns to Illuminated Targets

For monkey *M*, light-emitting diode (or "LED") targets were placed straight ahead and laterally towards the left at amplitudes of 37, 60, and 90° to evoke small to large head turns counter-clockwise in yaw. The purpose for having monkey *M* turn its head in the yaw plane at increasing amplitudes (30, 60, and 90°) was to increase task difficulty while evaluating the animal's posture for the normal and mBVH states. As stated previously, we hypothesized that the mildly impaired animal may be able to compensate for its loss, showing potentially no change or even decreases in trunk sway as head turn amplitude increased. By increasing target amplitude, we were able to increase balance-difficulty level for monkey *M*.

For monkey *S*, the animal implanted with the right-posterior canal prosthesis, targets were straight ahead (at 0°), or offset at ~40° oblique (counter-clockwise in yaw an upward in pitch along the left-anterior, right-posterior (LARP) plane) so that head turns between targets approximated the plane of the implanted right posterior canal. The main purpose for having monkey *S* turn its head in the LARP plane was due to the placement of the unilateral, right-posterior vestibular prosthesis. We aimed to provide a target location for the animal that would maximize modulation of the prosthesis during the animal's head turns. We hypothesized that monkey *S* would have decreased trunk sway when it turned its head in the sBVH + STIM-ON state (i.e., receiving prosthetic stimulation) compared to without in the sBVH state. Fig. 1a & b shows a schematic example of head turns between the visual targets for monkey *S*.

A manual switch was pressed by the experimenter to illuminate the targets in the different positions, and the monkeys were trained to turn their head between targets by providing a juice reward for correct performance. During test sessions, the time of the manual switch press was recorded as a step in the digital output (i.e., a value of either 0 (off) or 1 (on)). This was used to mark the onset of LED on in the head measurement data record. After the test session, each head turn from straight-ahead to the offset target were marked by the data analyst. The digital output aided in determining the head turn interval: the time just before and just after the head turn. Each head turn interval (or section) consisted of the following: start) the 0° target being illuminated and the animal facing forward; end) the offset target being illuminated and the animal turned its head. The initial maximum value of head yaw following the offset target being illuminated marked the end of the head turn interval.

Data

Measured output responses were the body movements of the animal and support surface reaction forces. The monkeys donned a tight fabric vest that held a small *position sensor* (minibird, Ascension Co., Burlington VT) on the back in a mid-sagittal position at the rostral-caudal level of the scapula base (to measure foretrunk motion) and also on the headcap (to measure head motion). The sensors measured angular and linear position (six degrees of freedom), sampled at a rate of 100 Hz. For monkey *M*, each of the four footplates was instrumented with tri-directional *force sensors* (ME-Meßsysteme GmbH, KD24S, Hennigsdorf, Germany), and force data were sampled at 200 Hz using Labview software (National Instruments Corporation, Austin, TX). Because force sensors where not calibrated at the time of monkey *S*'s experiments, force data was not acquired for monkey *S*.

Head and Foretrunk Parameters—The parameters of interest were the maximum displacements, or ranges of motion, (MAXD) for the head and foretrunk (Equation 1). In order to normalize the data based on head motion, a percentage movement of foretrunk roll or yaw relative to head yaw were also computed (Equation 2). The normalization described allowed for us to determine if the changes observed in each (individual) animal's trunk sway were robust in spite of each animal's intrasubject (i.e., individual) head turn variability. For this reason, we observed both absolute trunk movement, as well as trunk movement normalized by head movement, to determine if the changes we were observing were robust.

$$MAXD = \max(x(i)) - \min(x(i)) \quad (1)$$

where x(i) = position data for either the head or foretrunk within a given head turn section for sample number "i"

$$\text{nMAXD foretrunk roll} = \left| \frac{MAXD_{foretrunkroll}}{MAXD_{headyaw}} \right| 100\% \quad (2)$$

where $MAXD_{foretrunkroo}$ = maximum foretrunk roll displacement

$MAXD_{headyaw}$ = maximum head yaw displacement

Usable data—After all head turns to the target were identified in the measured data, *outliers* based on MAXD head yaw were excluded from usable data with the following method: 1) MAXD head yaw from all trials were pooled and the lower quartile (Q1) and upper quartile (Q3) means were determined, and 2) the outlier trials were defined as those with 3) MAXD head yaw roll less than Q1−1.5*(Q3–Q1) or greater than Q3+1.5*(Q3–Q1) (Tukey 1977).

For each platform configuration, the overall mean and standard error of each of the foretrunk parameters were calculated from the results of all the usable head turn intervals. For monkey *S*, there were ample usable head turn sections (i.e. sBVH: N = 70 usable *(9 unusable)* and sBVH + STIM: N = 78 usable *(17 unusable)*). For monkey *M*, there were many usable head turn sections (i.e. normal, 37°: N = 75 and mBVH, 37°: N = 40 usable; normal, 60°: N = 171

usable and mBVH, 60°: N = 122 usable; normal, 90°: N = 120 usable and mBVH, 90°: N = 54 usable).

Torque—For monkey *M*, vertical force data was used to compute the torque in roll, i.e., a measure of the animal's resistance to motion in the roll plane. The moment of a force is the turning tendency, or "torque", about an axis passing through a specific point. In this case, the moment was determined about a point "P" which was located halfway transversely (0.5 of the medial-lateral width, w) between the footplates and 0.4 of the anterior-posterior length, L, towards the front footplates longitudinally (Fig. 1c). Moments were computed about this location because it was the ground projection of the approximate location of the animal's center-of-mass (or "COM"). Since the animal exerted ~55–60% weight on the front footplates in quiet-stance and head turn experiments, the COM was more towards the front footplates. Furthermore, previous studies have shown the rhesus monkey trunk COM to be ~ 40% towards the proximal joint center (Vilenksy 1978). Since the animal had a more narrowed medial-lateral stance than anterior-posterior, greater imbalance was expected in roll. Thus, the rolling moment was determined.

The moment was calculated by computing the cross product of the respective moment arm with the footplate force vectors and is shown in Equations 3 through 6 below. The torque in roll is shown in Equation 6.

$$\overline{M}_p = \overline{r} \times \overline{F} \quad (3)$$

where r = distance vector, or moment arm

F = force vector

P = point from which moments were calculated

or in expanded form

$$\overline{M}_p = (0.4L\bar{j} - 0.5w\bar{i}) \times \left(F_{LF}\bar{i} + F_{LF}\bar{j} + F_{LF}\bar{k}\right) + (0.4L\bar{j} + 0.5w\bar{i}) \times \left(F_{RF}\bar{i} + F_{RF}\bar{j} + F_{RF}\bar{k}\right) + \ldots$$
$$(-0.6L\bar{j} - 0.5w\bar{i}) \times \left(F_{LH}\bar{i} + F_{LH}\bar{j} + F_{LH}\bar{k}\right) + (-0.6L\bar{j} + 0.5w\bar{i}) \times \left(F_{RH}\bar{i} + F_{RH}\bar{j} + F_{RH}\bar{k}\right) \quad (4)$$

where L = anterior-posterior distance between footplate centers

w = mediolateral distance between footplate centers

$\bar{i}$ = unit vector in the x-direction

$\bar{j}$ = unit vector in the y-direction

$\bar{k}$ = unit vector in the z-direction

$\overline{F}_{LF}$ = force vector on left fore (or anterior) footplate

$\overline{F}_{RF}$ = force vector on right fore (or anterior) footplate

$\overline{F}_{LH}$ = force vector on left hind (or posterior) footplate

$\overline{F}_{RH}$ = force vector on right hind (or posterior) footplate

The moment-component in roll:

$$(M_p)_{roll}=M_p\bar{j}=\left(-0.5w\bar{i}\times F_{LF}\bar{k}\right)+\left(0.5w\bar{i}\times F_{RF}\bar{k}\right)+\left(-0.5w\bar{i}\times F_{LH}\bar{k}\right)+\left(0.5w\bar{i}\times F_{RH}\bar{k}\right) \quad (5)$$

or in scalar form

$$(M_p)_{roll}=(+0.5w(F_{LF})_z)+(-0.5w(F_{RF})_z)+(+0.5w(F_{LH})_z)+(-0.5w(F_{RH})_z) \quad (6)$$

where “z” denotes earth vertical

Anchoring Indices—Anchoring indices (Amblard et al. 1997) have been used as a means of describing the relative angular deviations of a body segment relative to an inferior body segment (e.g. head relative to foretrunk) and is shown in Equation 7.

$$AI=\frac{\sigma_r-\sigma_a}{\sigma_r+\sigma_a} \quad (7)$$

where AI = anchoring index

σ_r = standard deviation of the relative angular distribution (with respect to axes linked to inferior anatomical segment)

σ_a = standard deviation of absolute angular distribution of segment considered

Anchoring index (AI) was utilized to determine the movement of one body segment relative to an inferior body segment for normal and vestibular-lesioned states. An AI < 0 would, in theory, indicate that the body segment was more stable relative to the inferior body segment than in space (i.e., en bloc motion), an AI > 0 would indicate that the body segment was more stable in space than relative to the inferior body segment, and an AI = 0 would indicate that the body segment was neither more stable in space nor relative to the inferior body segment. For both normal and mBVH states of monkey *M*, as well as sBVH and sBVH +STIM states of monkey *S*, head-foretrunk AI were determined in roll.

Results

We report the results from the two animals: monkey *M* used to study normal and mild vestibular hypofunction (mBVH) and monkey *S* used to study severe bilateral vestibular hypofunction with and without prosthetic stimulation (sBVH and sBVH + STIM-ON).

Below we consider in turn the effects of mild vestibular ablation on normal postural responses to head turns (monkey *M*) and the effects of prosthetic canal stimulation in the monkey with severe vestibular damage (monkey *S*).

From the VOR, we had observed that monkey *S* was more severely impaired than monkey *M*. The extent to which the lesion was bilateral was not known, however, the aminoglycoside lesion was presumed to affect both ears equally. Monkey *M* was relatively resistant to aminoglycoside ablation, as its roll VOR gain was only *m*ildly reduced by 21% (0.42 → 0.33) relative to normal. In contrast, monkey *S* had more a *s*evere ablation with its roll VOR gain *reduced* by 60% (0.58→ 0.23) relative to baseline. In monkey *S*, the unilateral prosthesis implantation was only to the right posterior canal. With the aid of the vestibular implant the VOR gain in monkey S *increased* by 47% (0.23→ 0.50) relative to the severely ablated state.

Head turns in Monkey M: Normal versus mild bilateral vestibular hypofunction (mBVH) states

Monkey *M* performed the head turn experiment in both the normal and the mBVH states. The main sequence plot (head velocity as a function of head displacement) is shown in Fig. 2 for head turns in monkey *M* for both normal and mBVH states. For peak (MAXD) head yaw, both normal and mBVH states show that MAXD yaw increased with increasing target amplitude (Fig. 3a). However, for all head turn amplitudes, for normal and mBVH states, the animal undershot the actual target position (i.e., the animal turned its head part of the way and then likely used eye movements to fixate on the target) as shown in Fig. 3a. Prior studies had shown that for target displacements > 40° the eye usually remains within ~ 35° of its center position (e.g., Bizzi et al 1971; Barnes 1981; Freedman and Sparks 1997; Guitton and Volle 1987; Roy and Cullen 1998). McCluskey et al. (2007) extended this finding showing that for normal rhesus monkeys eye position remains within this range for even larger gaze shifts (i.e., as large as 120°). For our experiments, we speculate that the animal was moving its eyes within this range (35° of center position). In comparing peak head movements for 60 and 90° targets, there were no significant differences between normal and mBVH states. However, MAXD for mBVH was significantly less than normal ($df = 71$, $t = -5.68$, $p < 0.001$) for the 37° target (i.e., the mBVH animal possibly used its eye movements to fixate on the small-amplitude target rather than turning its head).

In both the normal and mBVH sensory states, the animal's (yaw) head turns caused both the foretrunk and head to move in the same direction in yaw (towards the target). MAXD foretrunk roll was normalized by MAXD head yaw (which we call "nMAXD foretrunk roll") and was expressed as an absolute percentage (Fig. 3b). For the mBVH state, nMAXD foretrunk was significantly more than normal for the 37° target amplitude ($df = 75$, $t = 5.68$, $p < 0.001$). For the 60° and the 90° amplitudes, the animal's mBVH nMAXD foretrunk roll was significantly *less* than normal ($df = 223$, $t = -9.09$, $p < 0.001$ and $df = 96$, $t = -5.16$, $p < 0.001$, respectively). For the mBVH state, nMAXD foretrunk roll decreased as target amplitude increased.

Moments in roll—One of the behavioral goals of the animal's postural response is to control the COM and, since most of the rhesus monkey's body mass resides in the foretrunk, the foretrunk position and stability are directly related to this task. When the animal exerted the appropriate forces on the platform to oppose/counteract the head turn movements, COM stability was achieved. Fig. 4a displays the mean roll moments (or torques) about an approximate COM projection, for the offset head turn amplitudes.

Roll torques were computed by calculating the cross product of the moment arm vector (from the approximate COM projection to the center of each footplate) and the vertical ground reaction force vectors that were equal and opposite of the forces that animal was exerting on the balance platform footplates, such that a positive reaction roll torque indicated the animal was rolling to the right and negative reaction roll torque indicated the animal was rolling to the left. Increases in magnitude, or absolute value, of the moment meant that the animal was more resistant to motion in roll.

Changes in postural strategy between sensory states in monkey M: relative motion of body segments—Anchoring indices were used to characterize the relative motion of a superior (the head) to inferior body segment (foretrunk) for monkey *M* in the normal and mBVH sensory states. For the head turn experiments, head-foretrunk roll AI was < 0 but increased with target amplitude in both the normal and mBVH states (Fig. 4b). An AI < 0 indicated that the head was more stable relative to the foretrunk than in space. For the 60 and 90° target amplitudes, the mBVH roll AIs were significantly less than normal ($df = 89$, $t = -2.35$, $p < 0.05$; $df = 259$, $t = -2.95$, $p < 0.01$, respectively).

Head turns in Monkey S: Severe bilateral vestibular hypofunction (sBVH) and severe bilateral vestibular hypofunction plus vestibular prosthesis-stimulated (sBVH + STIM-ON) states

In the sBVH + STIM compared to the sBVH state for all three axes of motion (i.e., yaw, pitch, and roll), monkey *S* had significantly less head displacement (i.e., MAXD head yaw: $df = 128$, $t = -3.87$, $p < 0.001$; MAXD head pitch: $df = 110$, $t = -3.428$, $p < 0.001$; MAXD head roll: $df = 114$, $t = -9.42$, $p < 0.001$). The main sequence plot (i.e., head velocity as a function of head displacement) is shown in Fig. 5 for head turns in monkey *S* for both sBVH and sBVH + STIM states.

Foretrunk motions for a set range of head turn magnitudes—One behavioral consequence of the electric prosthetic stimulation was that monkey *S* turned its head less (Fig. 5). However, to control for the differences in head movement amplitudes and velocity, we focused our quantitative analysis of foretrunk sway when the head turns were similar in peak displacement and peak velocity. Both measures were used in setting the head movement criterion because the rate of the head turn, not just its displacement, could affect the animal's foretrunk sway. We examined the head turns ranging between 25 – 40° in counter-clockwise in yaw for both states (sBVH: N = 26; sBVH + STIM: N = 36).

Fig. 6 shows that these head turns were *insignificantly different* in peak velocity and peak displacement for both yaw and pitch (the predominant motions for the head turns in the LARP plane to the oblique target) for both sBVH and sBVH + STIM – ON states. However,

there were significant decreases in head roll displacement and velocity (i.e., head MAXD roll: df = 47, t = −7.43, p < 0.001; head MAXV roll: df = 49, t = −2.44, p < 0.05, respectively). Ideally, we had aimed to identify sections wherein head pitch, yaw, and roll displacements and velocities were insignificantly different between the two states. However, no such window could be identified for the given data set—although we observed a decrease in head roll for the sBVH + STIM – ON state, we could not account for this changes by simply selecting a different range of head turns without compromising the other parameters. However, for the selected 25 – 40° head turn range in yaw, we found that that head MAXD roll and foretrunk MAXD roll were not correlated (i.e., the coefficient of determination, R^2, was 0.0009 and the correlation coefficient, R, was 0.03). Since R is very close to zero, this indicates no, or very weak, linear correlation between head MAXD roll and foretrunk MAXD roll. In other words, for this range the decrease in foretrunk roll could not be simply attributed to the decrease in head roll.

The roll, pitch, and yaw foretrunk movements were also computed for the sBVH and sBVH + STIM-ON states for the above head turn range (Fig. 7). In comparing the foretrunk yaw movements sBVH + STIM-ON state relative to the sBVH state, there was a significant increase in foretrunk MAXD yaw (df = 47, t = −7.43, p < 0.001) shown in Fig. 7b, but an insignificant decrease in foretrunk MAXV yaw (Fig. 7a). In comparing the foretrunk pitch movements in the sBVH + STIM-ON state relative to the sBVH state, there was an insignificant difference in foretrunk MAXD pitch (Fig. 7d), but an obvious significant decrease in foretrunk MAXV pitch (p < 0.001) shown in Fig. 7c. There were significant decreases in foretrunk MAXD roll (df = 42, t = −2.55, p < 0.02) and foretrunk MAXV roll (df = 40, t = −9.49, p < 0.001) shown in Fig. 6e & 6f, respectively. The left panels in Fig. 7 show decreasing trends/significant decreases in foretrunk MAXV in yaw, pitch, and roll in the sBVH + STIM-ON state relative to the sBVH state.

Changes in postural strategy between sensory states: relative motion of body segments—In order to determine if there were changes in postural strategy between the sBVH and sBVH + STIM sensory states, roll AI was calculated (Fig. 8). For both sensory states, the AI was negative, indicating that the head was more stable relative to the foretrunk than in space (i.e., the foretrunk was being “carried with” the head). Since the animal was performing head turns to illuminated targets, this result was not surprising. However, the decrease in AI when the animal received prosthetic stimulation was insignificant.

Discussion

Our principal findings were that: a) mild vestibular ablation did not increase the trunk sway associated with head turns in the mildly impaired animal and b) the one-dimensional canal prosthesis reduced trunk roll associated for head turns in the severely impaired animal. This held true even when the amplitude and dynamics of the head turns between the two states (sBVH, sBVH + STIM) were comparable (i.e., for the windowed range of head turns as described above). Below we discuss these results in more detail and consider their potential implications regarding the potential postural effects of a vestibular prosthesis.

Effects of mild vestibular ablation

Comparing the normal and mBVH states, we found that sway actually decreased after mild ablation was induced. Our prior studies in the same animal studying sway during quiet stance (Thompson 2013) found a similar reduction in sway after mild vestibular ablation, and our modeling suggested that this reflected increased stiffness (e.g., muscle co-contraction) as the underlying mechanism used to compensate for the mild vestibular damage. In the current study, the mBVH animal showed increasing torque magnitude (or absolute value of torque) compared to normal for increasing head turn target amplitude (Fig. 4a). The increase in torque magnitude exerted by the animal in the mBVH sensory state presumably allowed it to “stiffen” (i.e., reduce its foretrunk body sway) compared to the normal state. This increased “stiffness” is consistent with previous results that show body or head displacements in bilateral vestibular-loss humans and cats leads to higher levels of tonic activity in the neck, foretrunk, and legs (Horak et al. 1994), and further is similar to the increased limb force we measured in the mildly ablated monkey during quiet stance (Thompson 2013). Furthermore, the decrease in AI in the mBVH compared to the normal states suggests a change in postural strategy, namely in the mBVH state the animal may have adopted a head-fixed-to-foretrunk strategy to compensate for its mild vestibular loss. This strategy has been previously described in human vestibular-loss subjects (Herdman 1994).

In summary, monkey *M*, with the mild ablation, had comparable/less trunk sway to its normal state. This may provide a possible indication that the compensation mechanisms used to stabilize the trunk in the setting of mild vestibular ablation. However, this strategy may have posed inadequate for monkey M if its vestibular damage were more severe.

Effects of prosthetic stimulation on severe vestibular ablation

When the severely ablated monkey received prosthetic canal stimulation in the plane of the head turn, foretrunk sway decreased even when controlled for changes in the head movements in the sBVH and sBVH + STIM states. Our observations suggest that the prosthetic electrical stimulation modulated by the animal’s angular head velocity may have partially restored information that was normally supplied by the intact canal and that this information was adequate to reduce postural sway during head turns (Fig. 9).

Previous studies in humans (e.g., Mergner et al. 1997) and in normal and labyrinthectomized cats (Stapley et al. 2006) have hypothesized that the combination of vestibular and neck afferent information contributed to trunk stability in space. It has been suggested that vestibular (“head-in-space”) inputs and neck proprioceptive (“head-on-trunk”) inputs are combined to calculate the position and velocity of the trunk relative to earth-based coordinates such as the line of gravity (“trunk-in-space”) (e.g., Mergner 1997). If this is correct, then the absence of either vestibular or neck proprioceptive information would lead to an erroneous estimate of trunk position. Intact cats, humans (and monkeys) receive both vestibular (head-in-space) signals and neck proprioceptive (head-on-trunk) signals. When neck proprioceptive signals are combined with vestibular signals, the result yields a reliable estimation of trunk orientation (Fig. 9a). Vestibular-lesioned test subjects, however, lack the head-in-space signal but are still receiving a reliable head-on-trunk signal. As a result, the

vestibular-loss subject estimates an erroneous trunk position (trunk-in-space) leading to imbalance and falls (Stapley et al., 2006) (Fig. 9b).

We propose that the electric stimuli delivered by the vestibular prosthesis partially restored information about head rotation to the severely ablated animal (Fig. 9c). Because of this, an animal in a severely vestibular-impaired state aided by a vestibular prosthesis (sBVH + STIM-ON) was able to obtain a more accurate estimate of foretrunk position (Fig. 9c), leading to reduced foretrunk sway (increased stability) in the sBVH + STIM-ON state compared to the sBVH state without stimulation. Because the rhesus monkey with severe bilateral vestibular loss exhibited a decrease in foretrunk roll when receiving vestibular prosthetic stimulation, we propose that the prosthetic electrical stimulation modulated by the animal's head velocity partially restored head velocity information. When the central nervous system integrated this information, it provided the severely-impaired animal more accurate head orientation cues than when the animal was without the stimulation. The more accurate estimate of head orientation allowed the severe vestibular-loss animal a better estimate of foretrunk position. This was observed as a reduction in foretrunk sway for the stimulated state (sBVH + STIM-ON) compared to the non-stimulated state (sBVH).

Our results suggest that an animal with mild vestibular impairment can compensate for their loss. However, implementation of a vestibular prosthesis in a severely vestibular-impaired rhesus monkey led to a more stable posture than without.

Acknowledgments

We thank Dr. Conrad Wall for advice on experimental design and James Lackner.

Grants

This work was supported by the National Institutes of Health (NIH) grant DC8362 to R.F. Lewis and by NIH Grant T32 DC00038 which supported L.A. Thompson.

References

Amblard B, Assaiante C, Fabre JC, Mouchnino L, Massion J. Voluntary head stabilization in space during oscillatory trunk movements in the frontal plane performed in weightlessness. Exp Brain Res. 1997; 114(2):214–225. [PubMed: 9166911]

Bach-y-Rita P, Kercel SW. Sensory substitution and the human machine interface. Trends Cogn Sci. 2003; 7:541–546. [PubMed: 14643370]

Barnes GR. Visual-vestibular interaction in the coordination of voluntary eye and head movements. Progress in oculomotor research. 1981:299–308.

Bizzi E, Kalil RE, Tagliasco V. Eye-head coordination in monkeys: evidence for centrally patterned organization. Science. 1971; 173(3995):452–454. [PubMed: 17770450]

Chiang B, Fridman GY, Chenkaii D, Rahman MA, Della Santina CC. Design and performance of a multichannel vestibular prosthesis that restores semicircular canal sensation in rhesus monkey. IEEE Trans Neural Syst Rehabil Eng. 2011; 19(5):588–598. [PubMed: 21859631]

Della Santina CC, Migliaccio AA, Patel AH. Electrical Stimulation to Restore Vestibular Function Development of a 3-D Vestibular Prosthesis. IEEE-EMBS 2005. 27th Annual International Conference of the. 2006:7380–7385.Engineering in Medicine and Biology Society, 2005

Dozza M, Chiari L, Horak F. Audio-Biofeedback Improves Balance in Patients With Bilateral Vestibular Loss. Arch Phys Med Rehabil. 2005; 86(7):1401–1403. [PubMed: 16003671]

Fitzpatrick RC, Day BL. Probing the human vestibular system with galvanic stimulation. Journal of Applied Physiology. 2004; 96(6):2301–2316. [PubMed: 15133017]

Freedman EG, Sparks DL. Eye-head coordination during head-unrestrained gaze shifts in rhesus monkeys. J Neurophysiol. 1997; 77(5):2328–2348. [PubMed: 9163361]

Fridman GY, Davidovics NS, Dai C, Migliaccio AA, Della Santina CC. Vestibulo-Ocular Reflex Responses to a Multichannel Vestibular Prosthesis Incorporating a 3D Coordinate Transformation for Correction of Misalignment. J Assoc Res Otolaryngol. 2010; 11(3):367–381. [PubMed: 20177732]

Guitton D, Volle M. Gaze control in humans: eye-head coordination during orienting movements to targets within and beyond the oculomotor range. J Neurophysiol. 1987; 58(3):427–459. [PubMed: 3655876]

Golub JS, Ling L, Nie K, Nowack A, Shepherd SJ, Bierer SM, Jameyson E, Kaneko CR, Phillips JO, Rubinstein JT. Prosthetic implantation of the human vestibular system. Otology & neurotology: official publication of the American Otological Society, American Neurotology Society [and] European Academy of Otology and Neurotology. 2014; 35(1):136.

Gong W, Merfeld DM. System design and performance of a unilateral semicircular canal prosthesis. IEEE Trans Biomed Eng. 2002; 49(2):175–181. [PubMed: 12066886]

Guyot JP, Sigrist A, Pelizzone M, Kos MI. Adaptation to steady-state electrical stimulation of the vestibular system in humans. Annals of Otology, Rhinology & Laryngology. 2011; 120(3):143–149.

Herdman, SJ. Contemporary Perspectives in Rehabilitation by Wolf SL. Philadelphia, PA: 1994. Vestibular Rehabilitation; p. 392

Horak FB, Shupert CL, Dietz V, Horstmann G. Vestibular and somatosensory contributions to responses to head and body displacements in stance. Exp Brain Res. 1994; 100(1):93–106. [PubMed: 7813657]

Judge SJ, Richmond BJ, Chu FC. Implantation of magnetic search coils for measurement of eye position: an improved method. Vision Res. 1980; 20:535–538. [PubMed: 6776685]

Lewis RF, Haburcakova C, Gong W, Lee D, Merfeld DM. Electrical Stimulation of Semicircular Canal Afferents Affects the Perception of Head Orientation. J Neuroscience. 2013; 33(22):9530–9535. [PubMed: 23719819]

Lewis RF, Haburcakova C, Wangsong G, Karmali F, Merfeld DM. Vestibuloocular Reflex Adaptation Investigated With Chronic Motion-Modulated Electrical Stimulation of Semicircular Canal Afferents. J Neurophysiol. 2010; 103(2):1066–1079. [PubMed: 20018838]

McCluskey MK, Cullen KE. Eye, head, and body coordination during large gaze shifts in rhesus monkeys: movement kinematics and the influence of posture. J Neurophysiol. 2007; 97(4):2976–2991. [PubMed: 17229827]

Merfeld DM, Haburcakova C, Wangsong G, Lewis RF. Chronic Vestibulo-Ocular Reflexes Evoked by a Vestibular Prosthesis. IEEE Trans Biomed Eng. 2007; 54(6):1005–1015. [PubMed: 17554820]

Mergner T, Huber W, Becker W. Vestibular–neck interaction and transformation of sensory coordinates. J Vestib Res. 1997; 7:347–367. [PubMed: 9218246]

Minor LB. Intratympanic Gentamicin for Control of Vertigo in Meniere's Disease: Vestibular Signs That Specify Completion of Therapy. Am J Otology. 1999; 20(2):209–219. [PubMed: 10100525]

Mitchell DE, Dai C, Rahman MA, Ahn JH, Della Santina CC, Cullen KE. Head movements evoked in alert rhesus monkey by vestibular prosthesis stimulation: implications for postural and gaze stabilization. PloS one. 2013; 8(10):e78767. [PubMed: 24147142]

National Institute on Deafness and Other Communication Disorders (NIDCD). Strategic Plan (FY 2006–2008). Available at: www.nidcd.nih.gov/StaticResources/about/plans/strategic/strategic06-08.pdf. Accessed May 20, 2010

Nie K, Ling L, Bierer SM, Kaneko CR, Fuchs AF, Oxford T, Rubinstein JT, Phillips JO. An experimental vestibular neural prosthesis: design and preliminary results with rhesus monkeys stimulated with modulated pulses. Biomedical Engineering, IEEE Transactions on. 2013; 60(6):1685–1692.

Peterka RJ, Wall C, Kentala E. Determining the effectiveness of a vibrotactile balance prosthesis. J Vestib Res. 2006; 16:45–56. [PubMed: 16917168]

Phillips C, DeFrancisci C, Ling L, Nie K, Nowack A, Phillips JO, Rubinstein JT. Postural responses to electrical stimulation of vestibular end organs in human subjects. Exp Brain Res. 2013; 229:181–195. [PubMed: 23771587]

Rogers MW, Mille ML. Lateral stability and falls in older people. Exerc Sport Sci Rev. 2003; 31:182–187. [PubMed: 14571957]

Stapley PJ, Ting LH, Kuifu C, Everaert DG, Macpherson JM. Bilateral vestibular loss leads to active destabilization of balance during voluntary head turns in the standing cat. J Neurophysiol. 2006; 95(6):3783–3797. [PubMed: 16554521]

Thompson, LA. Dissertation. Massachusetts Institute of Technology (MIT); 2013. A Study of the Effects of Sensory State on Rhesus Monkey Postural Control.

Tukey, JW. Exploratory Data Analysis. Addison-Wesley, editor. Reading, MA: 1977.

Tyler M, Danilov Y, Bach-y-Rita P. Closing and open-loop control system: Vestibular substitution through the tongue. J Integr Neurosci. 2003; 2(2):159–164. [PubMed: 15011268]

Vilenksy JA. Masses, Centers-of-Gravity, and Moments-of-Inertia of the Rhesus monkey (Macaca Mulatta). Am J Phys Anthrop. 1979; 50:57–66.

Wall C, Kos MI, Guyot JP. Eye movements in response to electric stimulation of the human posterior ampullary nerve. Annals of Otology, Rhinology & Laryngology. 2007; 116(5):369–374.

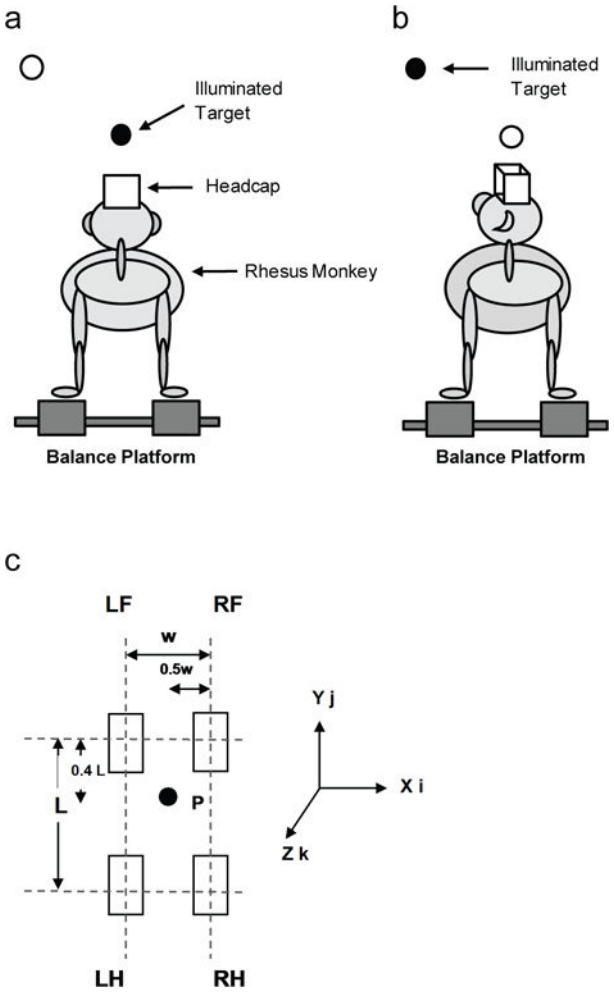

Fig. 1.

a & b) Schematic illustration of a monkey standing on the balance platform, with the head-fixed juice reward system focused on illuminated targets; c) Schematic of the top view of platform (without animal) for moment calculation. “LF” and “RF” denote “left-fore” and “right-fore”, respectively, and “LH” and “RH” denote “left-hind” and “right-hind”, respectively. Point “P” denotes the ground-projected, approximate location of the center-of-mass (COM). The location of “P” was halfway transversely between the footplates (0.5 of the medial-lateral width, w = 9 cm) and 0.4 of the anterior-posterior, or longitudinal length, L = 29 cm, towards the front footplates. For reference, earth-vertical, or yaw axis, “Z”, and earth-horizontal roll, “Y”, and pitch axes, “X”, are also shown with their respective unit vectors (k, j, and i)

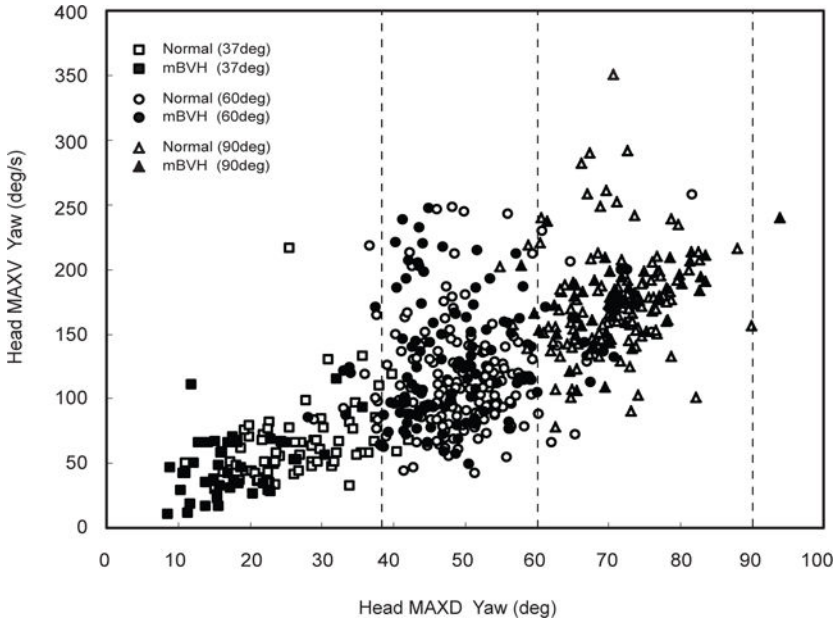

Fig. 2.

For Monkey *M* (37, 60, and 90° target amplitudes): Main sequence plot of head maximum velocity in yaw (or head MAXV yaw) as a function of head maximum displacement in yaw (or head MAXD yaw) for normal (white icons) and mBVH states (black icons); for reference, dashed lines shown are actual target locations

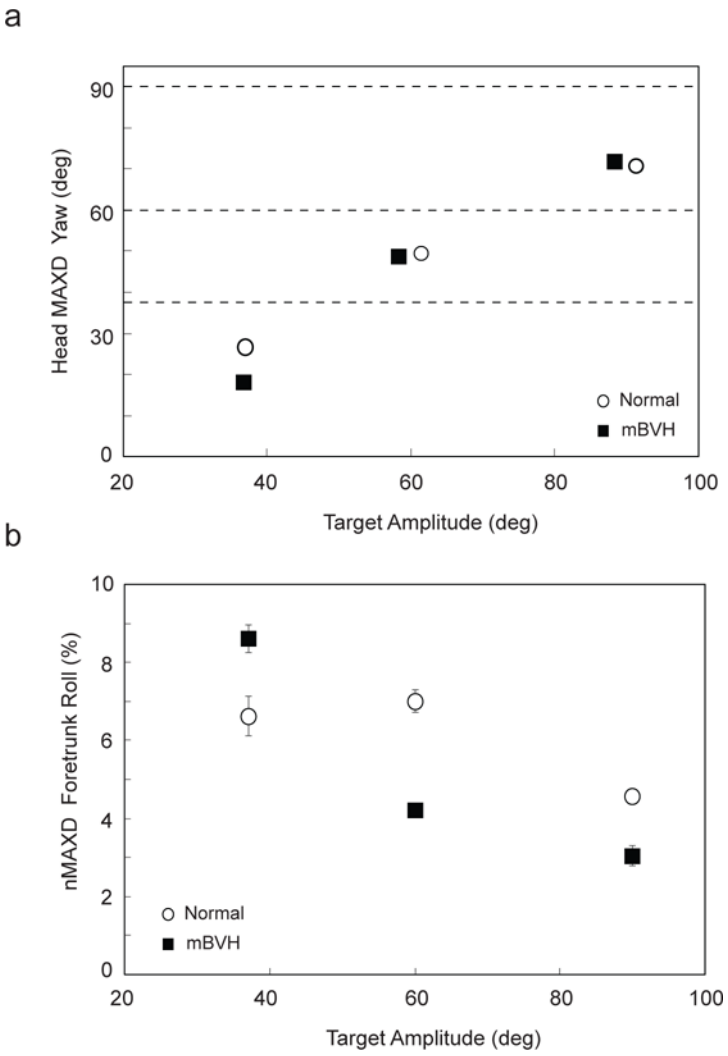

Fig. 3.

For Monkey *M* (37, 60, and 90° target amplitudes): a) MAXD Head yaw as function of target amplitude both normal (open circle) and mBVH (black square) states. Standard error bars are shown, but are very small and thus not visible; for reference, dashed lines shown are actual target locations; b) Foretrunk peak roll normalized by head peak yaw (or nMAXD foretrunk roll), as a function of target amplitude both normal (open circle) and mBVH (black square) states. Standard error bars are shown

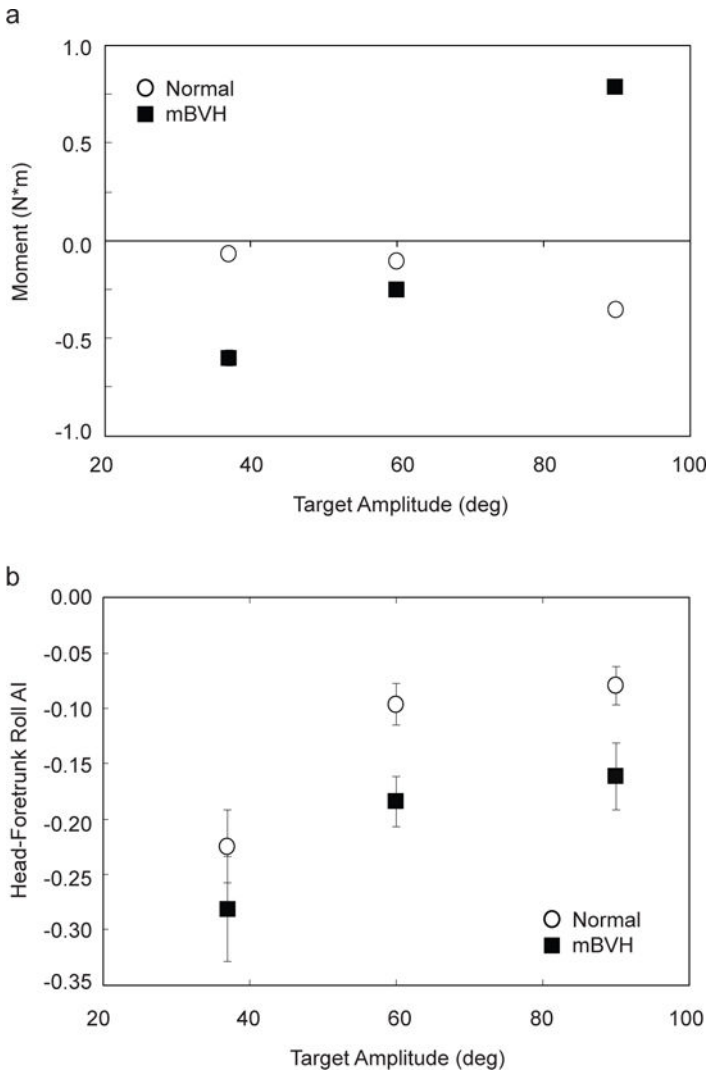

Fig. 4.

For Monkey *M* (37, 60, and 90° target amplitudes in counter-clockwise in yaw): a) Mean roll moments about the approximate center-of-mass (COM) projection as a function of target amplitude for both normal (open circle) and mBVH (black square) states. Standard error bars are shown; b) Head-foretrunk roll anchoring index (or "AI") with standard error bars shown both normal (open circle) and mBVH (black square) states

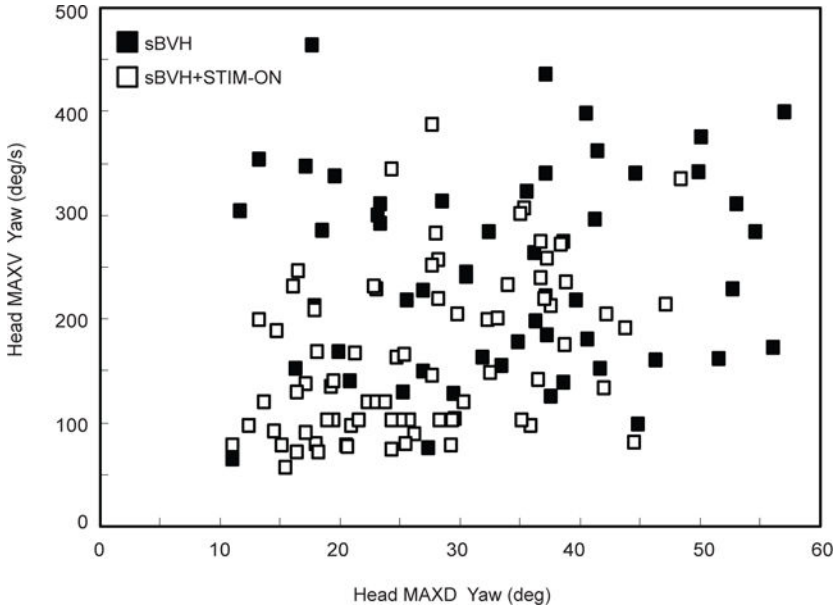

Fig. 5.

For Monkey *S* (40° oblique target amplitude (in LARP plane)): Main sequence plot of head maximum velocity in yaw (or head MAXV yaw) as a function of head maximum displacement in yaw (or head MAXD yaw) for sBVH + STIM (white icons) and sBVH states (black icons)

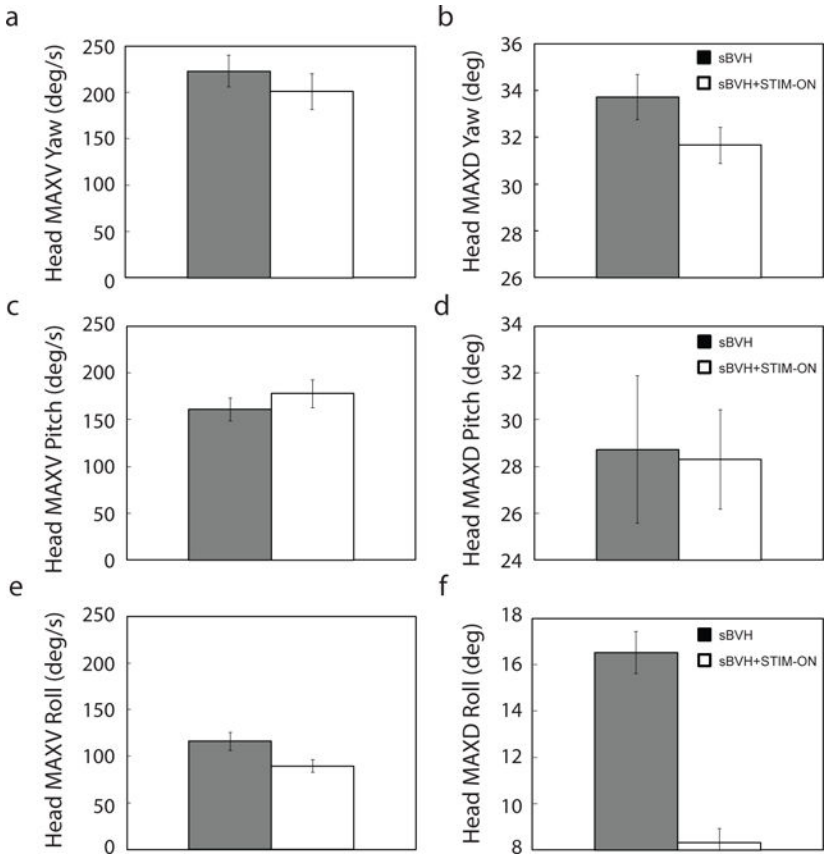

Fig. 6.

For Monkey *S* (40° oblique target amplitude (in LARP plane)) bracketed range in Fig. 4 (25 – 40° counter-clockwise in yaw, sBVH: N = 26; sBVH + STIM-ON: N =36): a & b) Head maximum velocity and displacement in yaw (i.e., head MAXV yaw (left) and head MAXD yaw (right)); c & d) Head maximum velocity and displacement in pitch (i.e., head MAXV pitch (left) and head MAXD pitch (right)); e & f) Head maximum velocity and displacement in roll (i.e., head MAXV roll (left) and head MAXD roll (right))

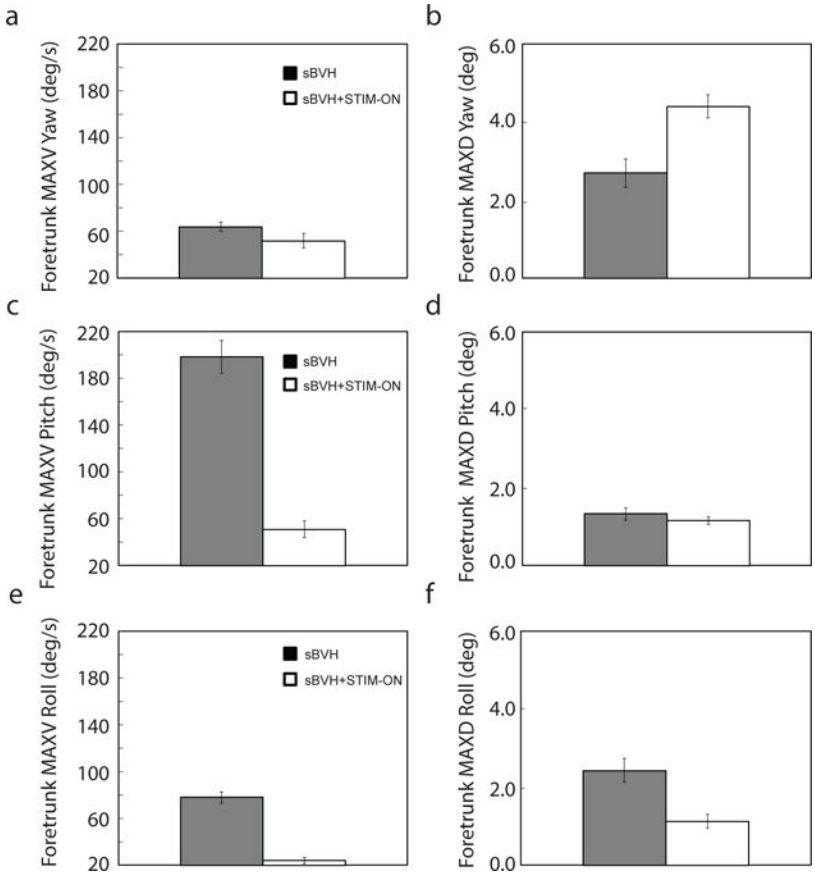

Fig. 7.

For Monkey *S* (40° oblique target amplitude (in LARP plane)) bracketed range in Fig. 4 (25 – 40° counter-clockwise in yaw, sBVH: N = 26; sBVH + STIM-ON: N =36): a & b) Foretrunk maximum velocity and displacement in yaw (i.e., MAXV yaw (left) and MAXD yaw (right)); c & d) Foretrunk maximum velocity and displacement in pitch (i.e., MAXV pitch (left) and MAXD pitch (right)); e & f) Foretrunk maximum velocity and displacement in roll (i.e., MAXV roll (left) and MAXD roll (right))

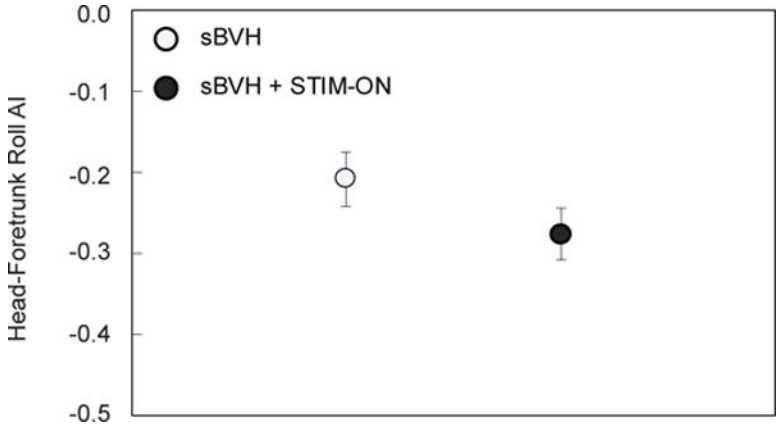

Fig. 8.

For Monkey *S*: Head-foretrunk roll anchoring index (or "AI") for sBVH (open circle) and sBVH + STIM-ON (closed circle) states with standard error bars shown

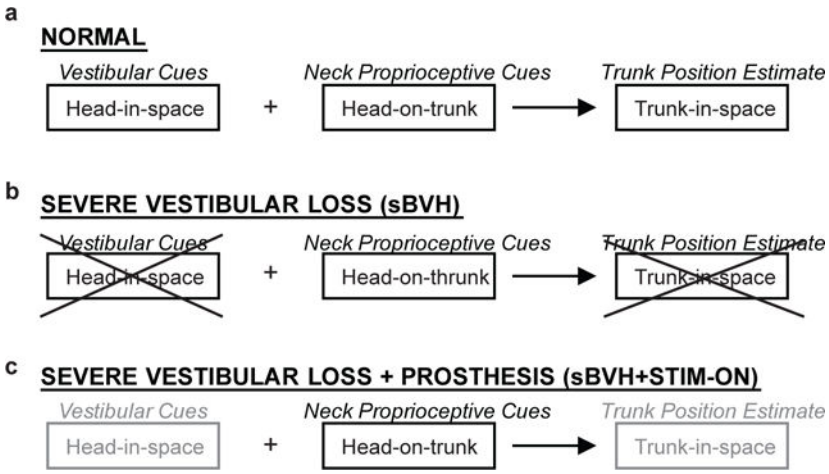

Fig. 9.

Schematic of a) normal; b) severe vestibular loss (sBVH); and c) severe vestibular loss assisted by prosthesis (sBVH + STIM-ON) trunk-in-space estimation. In panel c, light gray text is to indicate a partial restoration